Master Thesis

« Fluid Mechanics and Energetics »

Academic Year 2016-2017

Heat and mass transfer in dry and wetporous media

Saeid BAHRAMI EYNOLGHASI

Master Thesis performed at: Physics Institute of Rennes

Supervisors:

IPR: Edouard Canot

Ense^3: Robert Woumeni

Confidential thesis: YES ☐ NO ☒

Contents

Acknowledgment

I would like to express my gratitude to Edouard CANOT, my supervisor at IPR, for the time he dedicated to me, his explanations, and his kind assistance, which helped me adapt more quickly and easily to my new situation as a newcomer. I also extend my thanks to Robert WOUMENI, my supervisor at Grenoble INP, for his valuable guidance. Finally, I would like to thank the entire IPR team for their warm welcome.

1) Introduction

The aim of this research is to understand the process of heat transfer in a dry or wet porous medium. This study presents an experimental approach to studying heat and mass transfer in porous media. To accomplish this, we used white Fontainebleau sand, consisting of approximately spherical grains with a diameter of 200 µm. The experiment focuses on both dry and wet soils and is part of the ArPhyMat project: http://arphymat.univ-rennes1.fr/

One application of this project is in archaeology, where it contributes to a better understanding of the lives of prehistoric people. Archaeologists analyze the traces left by prehistoric people in order to gain insights into their way of life. For example, the remnants of a fire they used can provide interesting details about their lifestyle. The high temperatures of fires cause chemical reactions in the soil, which can be identified by changes in its natural color. Each temperature corresponds to a known color, and by determining the temperature (color) and depth, along with the soil's diffusivity, we can estimate the duration of the fire (Fig1). The traces of fires also provide information about their size, usage, and other properties, enabling archaeologists to gain a deeper understanding of the lifestyle of prehistoric people.

.

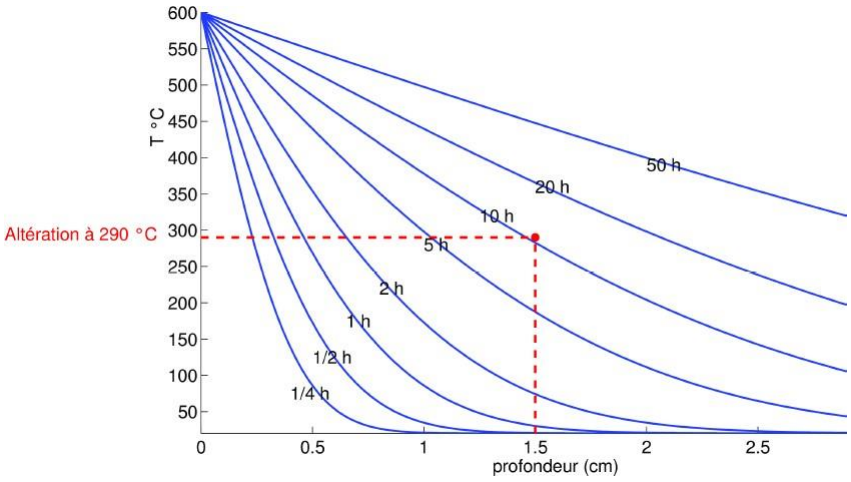

Figure-1

Another application of this project is in agriculture, specifically in the study of seed germination.
We need to determine the diffusivity to plot the curves shown in Fig1 or for other applications. It is known that thermal diffusivity can be calculated using the following formula:

$$\alpha = \frac{k}{\rho C_p}$$

However, measuring thermal diffusivity in porous media is a complex task due to the intricate nature of the conductivity process, especially in humid porous media. In such cases, different materials such as air, water, and grains with varying thermal conductivities are present. Additionally, the geometry of water between the grains is highly dependent on the amount of water in the mixture (Fig2). Consequently, the overall heat transfer in this scenario is a combination of microscopic heat transfers in multiphase media, where convection plays a significant role.

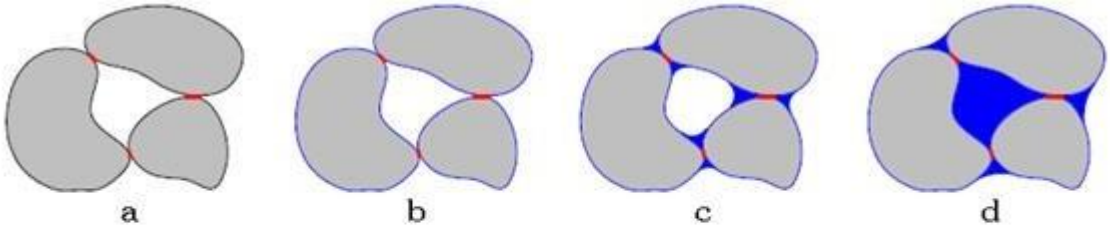

Sketch for dependence of thermal conductivity on water content in a coarse-textured porous medium. The contact between the grains is restricted to small regions (red) and the corresponding cross-sectional area is limiting for heat flow in a completely dry medium (a). As the water content increases, the pathways widen considerably thereby leading to a higher conductivity (b...d).

Figure-2 [2]

Thermal diffusivity in porous media is influenced by both mass transfer and heat transfer. In the case of dry soils, there is always a certain percentage of air present within the porous media. As the depth increases, this air becomes more compressed, leading to an increase in diffusivity. When we heat a dry porous media, the enclosed air expands and follows the heating path. In the case of wet media, heat transfer causes water to evaporate, resulting in a gradual increase in temperature during the evaporation process (our experiments demonstrated that evaporation occurs not at 100°C, but around 60°C). On the other hand, the produced vapor leads to rapid heating and higher diffusivity in the drier regions of the sand.

1-1) Equilibrium at a liquid-gas interface during temperature changes (Flat Plate)
To better comprehend the heat transfer phenomena in wet porous media, it is helpful to examine the behavior of the liquid-vapor interface under different pressures and temperatures.

As evident in (Fig3), there are two possibilities to consider when studying the behavior of the liquid-vapor interface.

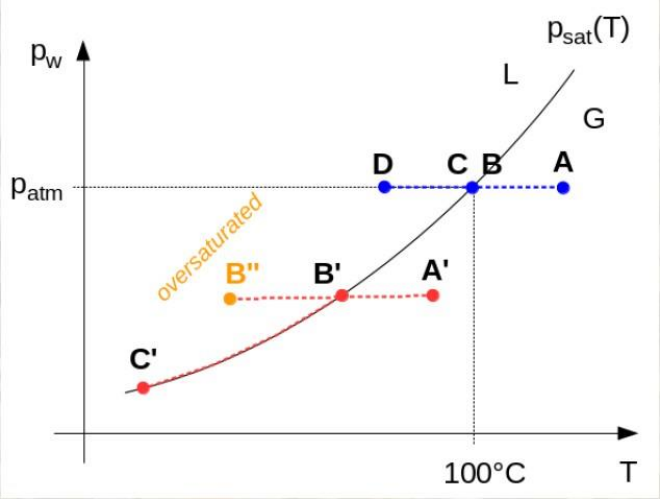

Figure – 3

1-1-1) The first case: a single component (water) represented by the blue line in Fig3

In this scenario, the pressure on the vapor and water solely arises from water molecules, with no air molecules present. At position "A," there is pure vapor. As the temperature decreases, the water molecules become closer together, but the pressure remains constant (e.g., atmospheric pressure). At point "B," the molecules are close enough, and condensation begins around small nucleation sites (such as dust particles or small cracks on the surface). From point "B" to point "C" (the saturated vapor region), both liquid and vapor phases coexist. Beyond point "C," all vapor is condensed, and at point "D," only the liquid phase remains.

1-1-2) The second case: two components (air and water) represented by the red line in Fig3:

In this case, the pressure on vapor and water comes from both water and air molecules. At point "A'," there is a vapor phase. As the temperature decreases, the vapor molecules become closer together. In this region, the pressure remains constant. At point "B'," two possibilities arise:

1. If there are no nucleation sites, the vapor molecules continue to come closer without any phase change, and the water molecules reach point "B'"" while being oversaturated.
2. If there are nucleation sites at point "B'," the water molecules start joining together and condense into water. Since the total pressure is due to both air and vapor molecules, the decrease in vapor molecules' number leads to an increase in the percentage of air molecules. This process occurs under constant total pressure. Consequently, the dew (condensation) temperature continues to decrease, and point "C'" follows the path of the saturated curve. As indicated in the section's title, all these phenomena are relevant to a flat plate. In the following section, we will examine the curved surface.

1-2) Equilibrium at a liquid-gas interface when temperature is constant (flat & curved)

The phenomenon of evaporation depends on the shape of the liquid's surface. In Fig4, two surfaces, one flat and one curved, are compared.

In the case of a flat surface, the vapor pressure immediately after the liquid surface, point "A," is equal to the saturation pressure. The vapor pressure in a region far from the liquid, represented by point "B," is lower than the pressure at "A." Over time, as indicated by the blue arrow in the chart, the pressure at point "B" increases due to more liquid evaporating, moving toward point "A." When point "B" reaches point "A," the system reaches equilibrium, and no further evaporation occurs.

However, for a curved surface, according to the Kelvin Equation, the vapor pressure at point "A'" (immediately after the liquid surface) is lower than the saturation pressure:

$$\frac{P_{va}}{p} = \exp\left(\frac{K\sigma V}{R\,T}\right)$$

$$\overline{P_{sa}}_{t}$$

In this formula:
σ = Surface tension
V= molar volume of the liquidR= universal gas constant
T= temperature

And K is depended on the radius of the curve.Flat interface: k = 0 $\rightarrow P_{vap} = P_{sat}$ (T)
Convex interface: k > 0 (cloud droplet: oversaturated)
Concave interface: k < 0 (under saturated)

As time passes, as shown by the red arrow in the chart, the vapor pressure at point "B'" increases due to liquid evaporation, causing a decrease in the amount of liquid. However, because the liquid is in a conical gap with a concave surface, as the liquid evaporates, the surface becomes more curved, changing the value of "K" (a constant in the Kelvin Equation). Consequently, the vapor pressure at point "A'" decreases. Eventually, "A'" and "B'" will reach a specific pressure below the saturated pressure, and further evaporation will cease. This is why the soil remains wet for a longer time in situations where the weather is not at the saturated vapor pressure.

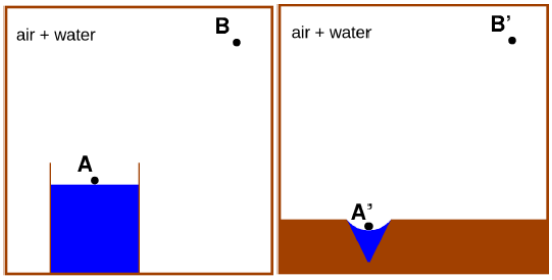

Figure -4(a)

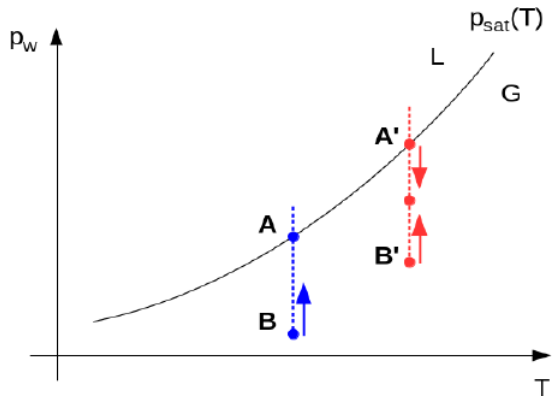

Figure – 4(b)

1-3) Heating humid soil

One aspect of this research involves studying the transfer of heat and mass in moist porous media. In this section, we will examine the changes in humidity and pressure in wet sand as it is heated from the surface.

For our experiments, we used a box filled with wet sand and applied a uniform heat flux to the surface of the sand. The change in humidity and pressure within the porous media was first modeled by Min & Emmons in 1972. Their model demonstrated, both experimentally and theoretically, that a temperature gradient causes humidity to migrate towards the colder region through evaporation and condensation. This phenomenon is commonly known as the "heat pipe effect."

Although the equations developed by Min & Emmons are clear, understanding the boundary conditions, particularly between the dry and wet zones, is challenging. Only a few other researchers have utilized their approach, and the accuracy of the complete set of equations, especially for non-stationary cases, has not been proven.

The EWGM model (Evaporation in Wet Granular Media) developed by Edouard Canot successfully reproduced a similar effect by using modern and accurate numerical algorithms to solve the entire set of equations. The results of the EWGM model are presented in Fig5, where different colors represent different time intervals. The red color indicates the starting time, while the blue color indicates the ending time. In Fig5, we can observe that at each time interval, the curve begins in the dry region of the porous media, where the liquid fraction is zero. Immediately after this region, the humidity increases to its maximum value in the wet sand. As we move deeper into the wet sand, the humidity gradually decreases until it reaches a constant value.

The locations with maximum humidity at specific times, along with their corresponding pressures, are indicated by dark points in Fig5. Additionally, we can observe that the pressure at these points is also the highest among all depths of the wet sand.

This phenomenon can be explained by considering the vapor that evaporates just below the dry region. This point receives the maximum amount of vapor because there is a larger amount of wet sand below it (the issue lies in the dimensions and the fact that vapor can only move towards the surface of the sand). In the lower parts, evaporation occurs at temperatures below saturation (as mentioned in section 1-1-2). However, since the entire wet sand is below the saturation temperature (during the experiments, we observed that the wet sand dried out at around 60°C), a portion of this vapor will always condense as the height increases. As a result, the humidity of the sand will increase until it reaches the region directly below the dry part, which is where the highest humidity is found.

As mentioned earlier, as the height increases, the wet sand receives more vapor, causing the pressure to increase along with the humidity (the vapor pressure adds to the total pressure). Just before the dry region, the pressure reaches its maximum. After this point, the pressure decreases with a constant slope, which is due to the pressure drop as the vapor moves towards the outside through the porous media.

As time passes, the amount of vapor increases due to the rising temperature. This increase in vapor leads to an increase in the liquid fraction and pressure in all wet areas, including the wet region at different heights. This trend continues until a certain point in time, which is indicated by the dark points in Figure 5. At this point, the liquid fraction in the soil starts to decrease due to prolonged evaporation. As a result, the amount of evaporated vapor and subsequently the amount of condensed vapor also decrease. The humidity curves decrease at a faster rate compared to the pressure curves because the condensing process decreases as the temperature in the wet soil increases over time.

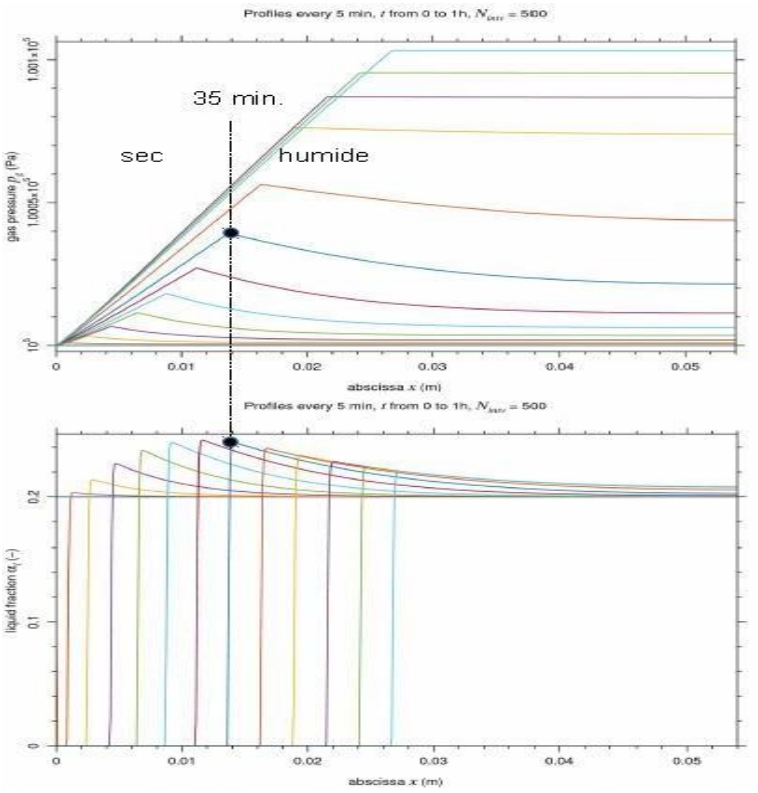

Figure- 5

1-4) Main tools and methodologies:

To conduct the experiments during this internship, we utilized two different systems. The first system, referred to as the "square box," consisted of a large cubic metal box (refer to Figure 6). Inside the box, we placed fine-grained sand particles measuring 0.2 mm in diameter. The horizontal surface of the box was heated by a large electrical heater (30 cm in diameter). Multiple thermocouples were positioned inside the box to measure and record the temperature using LabView software. However, due to non-uniform temperature distribution on the surface of this system, we developed a second system for conducting the majority of our experiments.

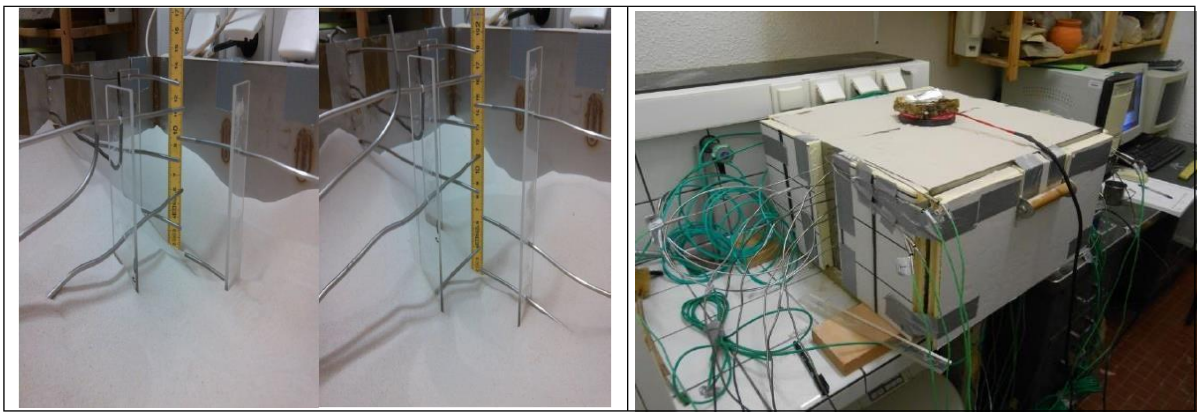

Figure - 6

The second system, depicted in Figure 7, is known as the "cylindrical box." It is smaller in size compared to the square box. The cylindrical box has the capability to contain either humid sand, water-saturated sand, or a two-layer porous medium. The two-layer porous medium consists of a lower layer saturated with water and an upper layer that is only wet. Temperature measurements in this system were obtained using a dozen vertical thermocouples that were fixed at the bottom but easily adjustable in terms of depth. Similar to the first experiment, all the collected data were recorded using LabView software.

Fig - 7

1-5) Models:

The HeMaTiS code (Heat and Mass Transfer in Soils) incorporates different physical models. The first model is the dry model, which employs the conventional transient heat equation in either one-dimensional (1D) or three-dimensional axisymmetric (3D-axi) configurations. However, in this model, the thermal properties of the air inside the porous medium are temperature-dependent.

$$\vec{\nabla} \cdot \left(-k \vec{\nabla} T \right) = q_{gen} - \rho c \frac{dT}{dt}$$

$$-k \vec{\nabla}^2 T + \rho c \frac{\partial T}{\partial t} = q_{gen}$$

$$\vec{\nabla}^2 T - \frac{1}{\alpha} \frac{\partial T}{\partial t} = -\frac{1}{k} q_{gen}$$

In our case, since there is no internal heat generation within the mass volume, the equation mentioned earlier will be modified as follows:

$$\boldsymbol{\nabla^2 T} - \frac{1}{\alpha} \frac{\partial T}{\partial t} = 0$$

Our objective is to determine the optimal α (diffusivity) that will yield numerical temperature values, at various depths and over time, closely matching the measured temperatures.

The second model addresses heat and mass transfer in an unsaturated porous media, which considers the phase-change behavior of water. This research also includes an experimental component, where the obtained results are used in numerical models to determine the diffusivity of the porous media. Furthermore, the experimental results will be utilized to compare and analyze the outcomes of the experimental and numerical approaches. The aim of this internship is to conduct the experimental part of the research in both dry and wet scenarios.

Detailed description of the problem & methodology:

During this internship, numerous experiments were conducted using both dry and wet sand. The following sections provide a detailed explanation of the numerical and experimental aspects of the research.

2-1) Numerical part:

The numerical model aims to estimate the temperature distribution within the porous media at different

depths by determining the most accurate diffusivity value for the media. Two models are employed for dry and wet sand, respectively. In these models, the governing equations are solved to calculate the temperature distribution within the sand at various locations. For humid soil, the evaporation of water (due to phase change) must also be considered in the calculations.

If all parameters in the governing equations are known, these equations can be directly solved. Such problems are referred to as forward problems. However, if not all parameters in the governing equations are known, it becomes necessary to solve inverse problems. In our case, since the diffusivity of the porous media is unknown, we employ thermal properties estimation to solve the inverse problem.

2-1-1) Inverse problem:

Numerous numerical techniques have been proposed for solving inverse problems. In this research, the following approach is utilized:

Initially, a custom Fortran code, developed by Edouard CANOT, is employed to solve the governing equations using an initial diffusivity value (α). This step involves solving the forward problem to obtain temperatures at different positions within the sand. These temperatures, obtained from the forward problem, are referred to as synthetic temperatures. In the subsequent step, the code subtracts the measured temperatures from the experiments from the synthetic temperatures, creating an error function based on the absolute value of the differences. This error function, which is dependent on the diffusivity value, is minimized using the Levenberg-Marquardt Method. The diffusivity value corresponding to the minimum of this function is defined as the best estimation for α, and the calculated temperatures associated with this diffusivity value are the output of the inverse problem. It's worth noting that due to variations in air density with depth and changes in the conductivity and thermal capacity of water and/or air with temperature (which is dependent on depth), the diffusivity of the porous media varies with depth in both wet and dry cases. Consequently, the experimental temperatures at different depths do not exactly match the calculated temperatures from the inverse problem.

2-2) Experimental part:

2-2-1) Square box:

For collecting experimental data, the square box (refer to Figure 6) was utilized in the initial experiment. Inside this box, thermocouples were installed at different heights. Glass plates were used to fix these probes at their designated positions. The glass plates had multiple holes at different heights where the probes were placed and secured, ensuring they remained at the desired positions. Glass was chosen as the material for these support plates because its conductivity is closest to the soil used in the experiments, minimizing its impact on the experiment. The square box was heated by a plate with spiral electrical wires functioning as a heater. After conducting several experiments and monitoring the recorded temperatures from the probes, it was observed that the temperature distribution on the surface of the sand was non-uniform due to the shape of the heater. It was noted that the non-uniformity in the temperature distribution increased over time, indicating that the non-uniform heat flux, caused by the constant power output of the heater, contributed to the growing non-uniformity of temperatures. Even after the temperatures reached a constant value, the non-uniformity persisted as the non-uniform heat energy continued to be added to different parts of the heated domain. This phenomenon, observed in numerous experiments using different systems and heaters, can be explained by considering the constant heat flux

of the heaters. The non-uniform heat flux, combined with increasing temperatures, leads to a non-uniform temperature distribution. Unlike cases without heat flux, where a non-uniform object would eventually reach a uniform temperature distribution over time, the presence of non-uniform heat flux prevents the object from reaching uniformity over time.

2-2-2) Cylindrical box:

In order to address the issue of achieving a uniform temperature distribution on the surface of the sand, which is a crucial boundary condition in the numerical part of the research and necessary for obtaining accurate results for use in the numerical code, we modified the experimental setup and utilized the cylindrical box (refer to Figure 7). Inside this box, there are 10 thermocouples positioned at different depths, enabling us to measure the temperature at various levels within the sand. The heater component in this new box differs from the previous rectangular box. Instead of direct contact heating, this heater employs infrared waves to heat the surface of the sand.

After conducting tests with this new heater and capturing infrared images of the sand's surface, it was observed that the temperature distribution on the sand's surface was non-uniform due to the shape of the heating component, specifically the two curved rods (refer to Figure 8). In the infrared image (Figure 8), it is evident that the heated part of the sand is not centered because the top half of the heating rods, which are the only parts capable of heating, are not positioned at the center. As a result, significant non-uniformity in the heated part of the sand is observed, represented by different colors in the image. The corresponding temperature values for each color are indicated in Celsius on the color bar.

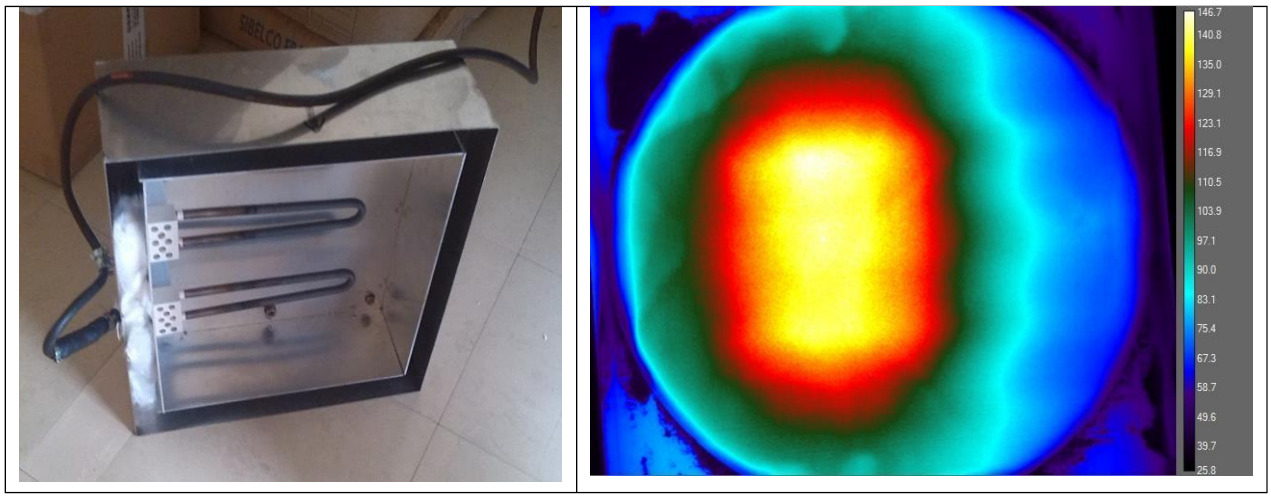

Figure -8

2-2-3) Cooling and heating with a black plate:

In order to address the non-uniform temperature distribution observed on the surface of the sand, an experiment was conducted to determine if using a metal plate with high conductivity could

achieve a uniform temperature distribution. Obtaining a uniform temperature under the area covered by this metal plate is beneficial and can be utilized as a boundary condition in numerical modeling. In this scenario, the governing equations need to be solved in two dimensions, and the isothermal lines will resemble a hemisphere.

Figure 9 illustrates the result of a two-dimensional numerical model for dry sand. In this model, there are 200 meshes in the "r" direction (radius) and 200 meshes in the "Z" direction (depth). The temperature distribution in the "r" direction is assumed to be symmetrical, with "r" starting from the center of the circular plate. The model demonstrates that the temperature of the plate remains constant and uniform. Additionally, the isothermal lines exhibit a hemisphere-like shape (as the depth increases, the shape of the isothermal lines becomes more similar to a hemisphere). In Figure 9, the white line indicates the region where the temperature reaches 100 degrees.

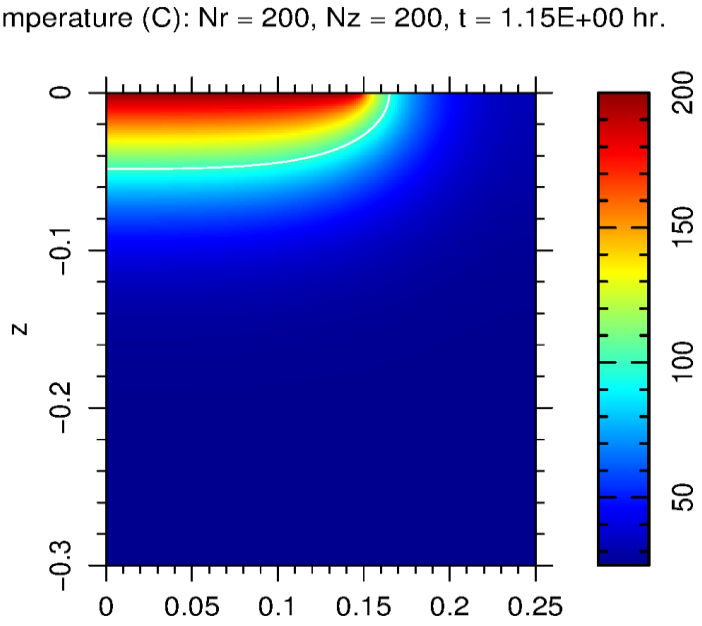

Figure – 9

After heating the surface of the sand and capturing an infrared photo, a circular black metal plate was placed at the center of the sand surface. As anticipated, during the cooling process, the surface temperature began to exhibit a more uniform distribution. However, due to the presence of the plate, it was observed that the center of the sand, specifically the area where the plate was located, had a higher temperature compared to other regions. A circular region with an approximately uniform temperature distribution was formed. The corresponding pictures are depicted in Figure 10.

In the final step (third picture), the infrared image gives the impression that the temperature of the plate is higher than the surrounding areas on the sand. However, this observation is misleading because of the following reason: the metal plate has a dark appearance while the sand is white. Consequently, the emissivity of the plate is higher than that of the sand. The infrared camera used for temperature

measurement is calibrated for objects with an emissivity value of one. As a result, it is unable to accurately measure the true temperature of the sand, leading to the discrepancy in the measurement.

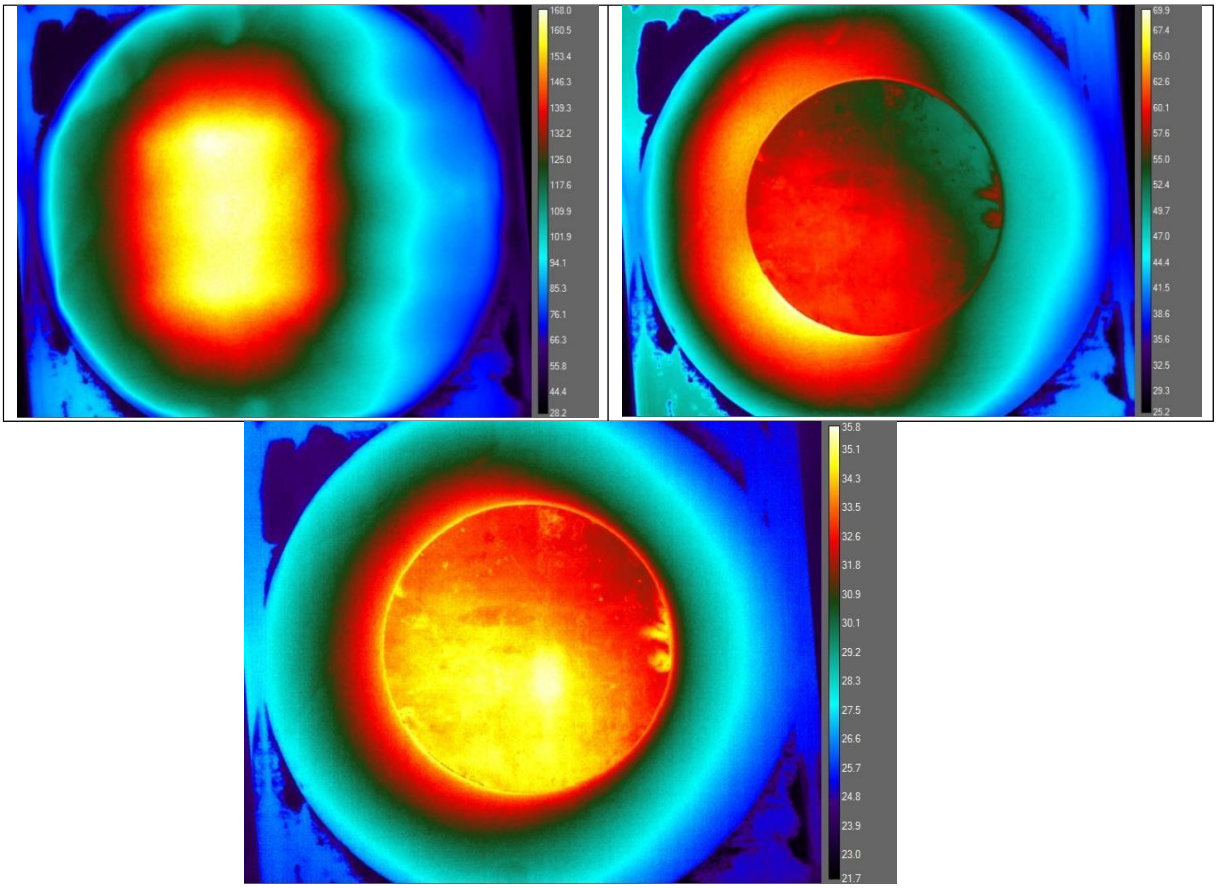

Figure -10

After conducting the previous experiment in an attempt to achieve a uniform temperature during the heating process, we proceeded by using the same plate and heating the surface of the sand. Two infrared photos were taken at different times during the heating process. The heater cap of the box was temporarily removed to capture the photos and then put back in place. However, as evident in the photos depicted in Figure 11, the temperature distribution could not achieve uniformity over time. This lack of uniformity can be attributed to the non-uniform heat flux mentioned in section 2-2-1.

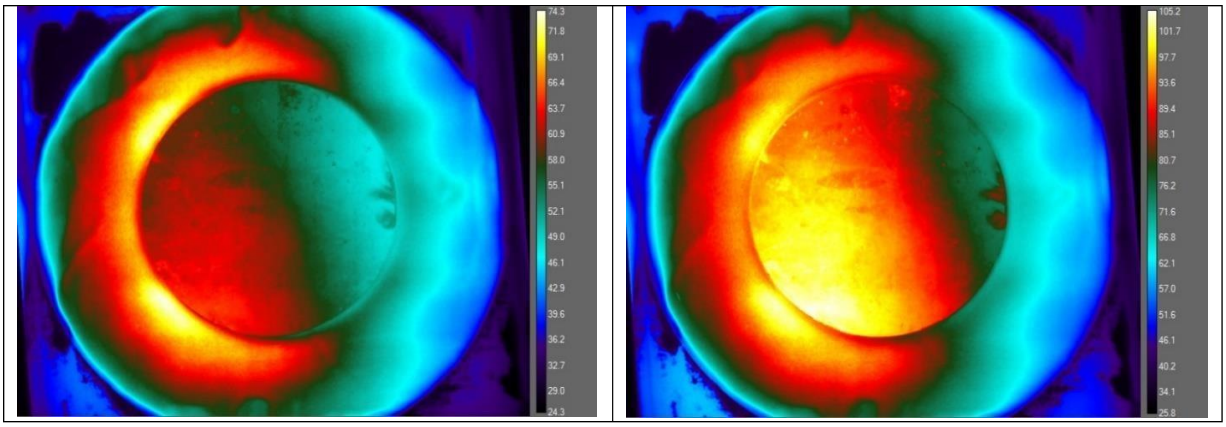

Figure -11

2-2-4) Using aluminum foil

we attempted to achieve a uniform temperature distribution by using aluminum foil to cover the entire surface of the sand, except for the central area where the metal plate was located. The reflective surface of the aluminum foil was expected to reflect the infrared radiation, allowing only the metal plate to receive the infrared energy. It was hypothesized that due to the high conductivity of the metal plate, the heat energy would quickly distribute within the plate, leading to a uniform temperature. In this new experiment, the heater cap of the box and the aluminum foil were periodically removed every few minutes, and an infrared photo was taken. The results, shown in Figure 12, clearly indicate that only the central part (the plate) was heated. As time progressed, as predicted in our model (Figure 9), a hot layer around the plate began to expand (depicted in pink color). However, some unusual patterns were observed in the infrared photo of the plate in Figure 12. These patterns persisted during the temperature increase, as well as after cutting off the heat flux and during the cooling phase. It was determined that these patterns were likely caused by the poor quality of the plate's color. The quality of the color coating affects the emissivity of the plate and can result in such phenomena. To address this issue, the plate was repainted with a uniformly black color that is resistant to high temperatures.

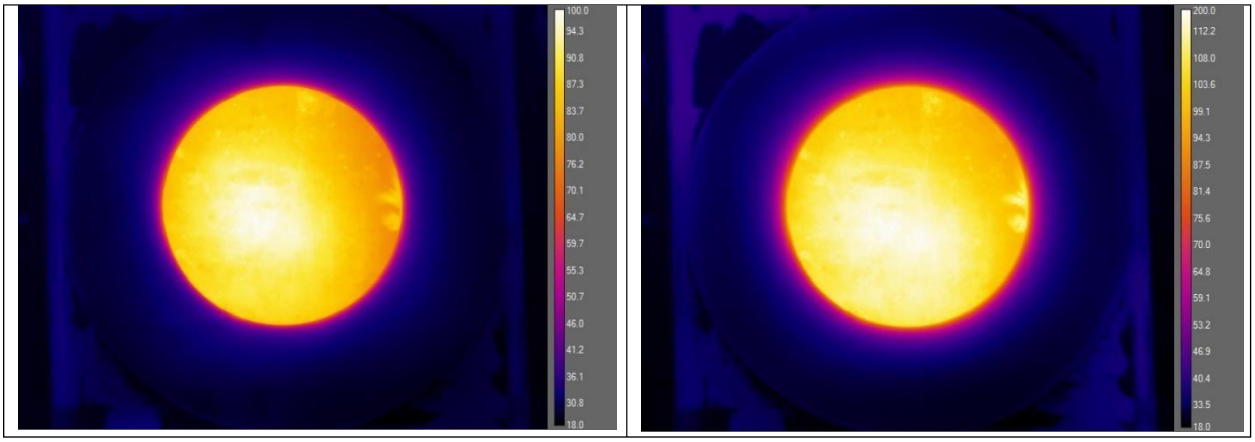

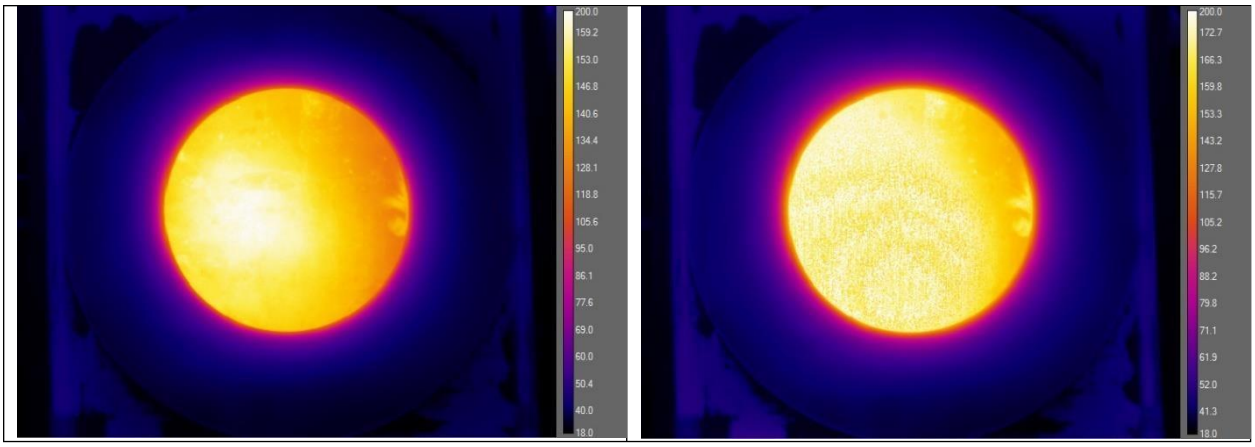

Figure -12

2-2-5) Testing the accuracy of infrared camera

As mentioned earlier, due to the presence of unusual patterns in the infrared photos, it was necessary to conduct an experiment to test the accuracy of the infrared camera before proceeding with painting the metal black. For this purpose, two small metal pieces were painted, one with a black color and the other with a heat-resistant color. These two pieces of metal were fastened together, with a thermocouple placed between them (refer to Fig13). After heating the metal pieces and capturing an infrared photo, it was observed that the temperature indicated by the thermocouple matched the temperature measured by the infrared camera. This experiment confirmed the accuracy of infrared measurements for surfaces with black colors (emissivity = 1).

In the subsequent step, the circular metal plate was painted with a high-quality black color, and then it was heated. As shown in Fig14, the previous unusual patterns seen in the previous photos were eliminated, and the temperature distribution on the circular plate appeared to be approximately uniform.

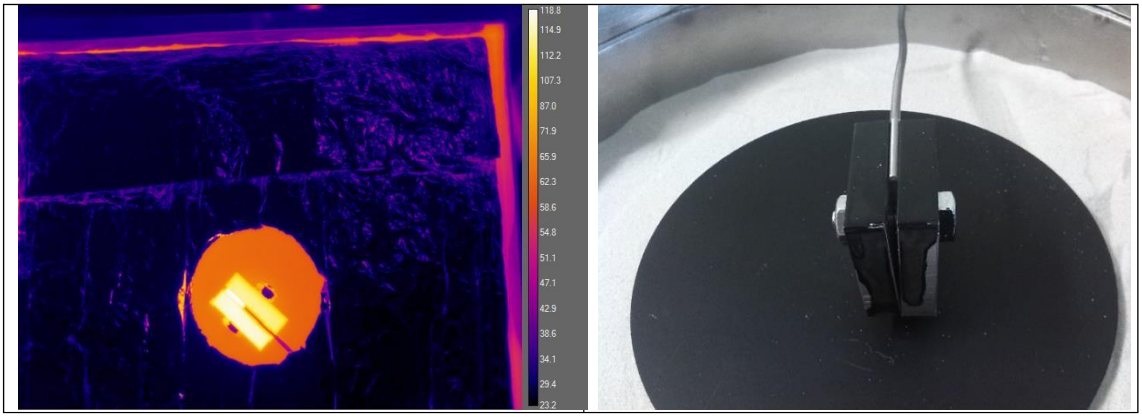

Figure -13

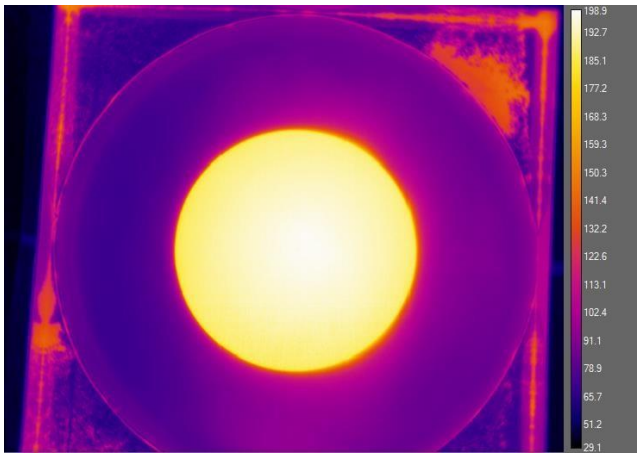

Figure -14

2-2-6) Investigation on the uniformity of temperature under the circular plate

As depicted in Fig14, the use of aluminum foil resulted in relatively homogeneous temperature distribution on the surface of the metal plate. This suggests that in previous experiments, when strange patterns were observed in the infrared photos of the plate, the surface temperature was relatively uniform (after the plate was painted, the issue of strange patterns was resolved). However, to further investigate the uniformity of temperature under the metal plate and on the surface of the sand (where a uniform temperature distribution is required for our models), another experiment was conducted.

In this experiment, the aluminum foil and the metal plate at the center of the surface were used to achieve a uniform temperature on the surface of the plate (similar to previous experiments). Inside the sand-filled box, ten thermocouples were installed, with their tops in contact with the plate's surface (exactly at the sand's surface). Subsequently, the surface of the box was heated. Fig15 shows an infrared photo of the metal plate after the heating process. The locations of the thermocouples beneath the metal plate and the temperatures they measured are also indicated in the temperature contour. It can be observed that unlike the surface of the metal plate, the temperature measured by the thermocouples exhibits significant differences. For further investigation, the metal plate was removed, and an infrared photo was taken of the sand's surface (Fig16).

As evident in Fig16, during the removal of the metal plate, some sand was also removed from the surface, resulting in a non-circular infrared photo. After capturing the infrared picture, temperature contours were drawn in Matlab, and the temperatures measured by the thermocouples were written at their respective locations on the contours. Since the emissivity of the sand is uniform, it was expected that the temperatures of the thermocouples would be the same along the same contour line (the part where sand was removed from the surface can be disregarded for interpretation). Contrary to expectations, Fig16 shows a relatively large difference in temperatures of thermocouples along the same infrared temperature contours.

Before drawing any conclusions, an experiment was conducted to ensure the accuracy of the thermocouples. All ten thermocouples in the box were placed inside a container of hot water to compare their temperatures and differences. The result of this experiment indicated that all thermocouples measured the same temperature, confirming their accuracy.

With confidence in the accuracy of the thermocouples, two conclusions were drawn from the results in Fig16:

Firstly, it was observed that despite the relatively uniform temperature in the infrared photos, the temperature distribution on the surface of the sand was not yet uniform.

Secondly, it was understood that the reason behind the relatively uniform temperature in the infrared photos of Fig15 and Fig16 is that immediately after removing the heater cap, a very thin layer of sand or metal becomes uniformly heated. This top layer with a uniform temperature causes the infrared photos to exhibit a uniform temperature distribution. However, due to non-homogeneous heat flux, the temperatures in the inner layers cannot immediately become uniform after the heating process is stopped. As demonstrated by the thermocouples in Fig15 and Fig16, the temperature is not uniform at any location during the heating process.

In Fig16, it can be observed that the thermocouples exhibit lower temperatures in the infrared photo. This phenomenon is due to the high conductivity of the thermocouples compared to other parts, causing them to cool down faster than other components.

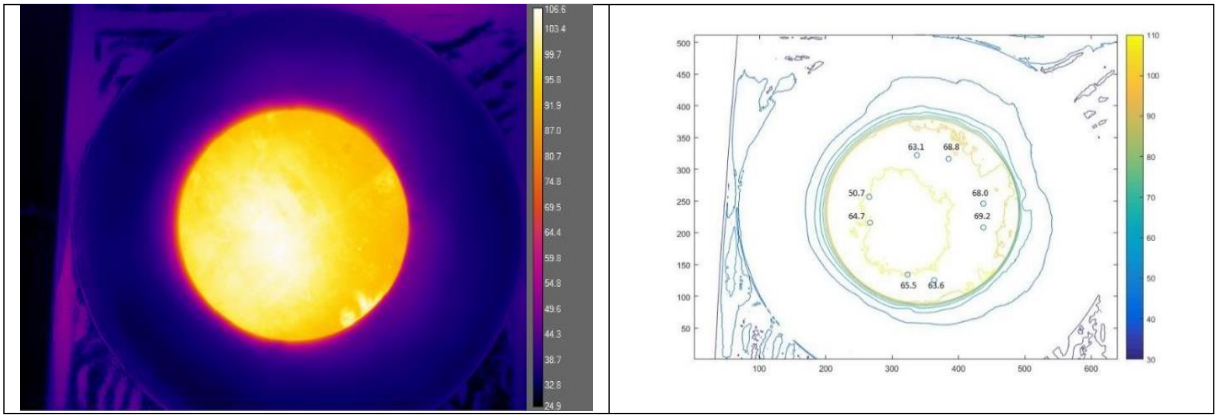

Figure -15

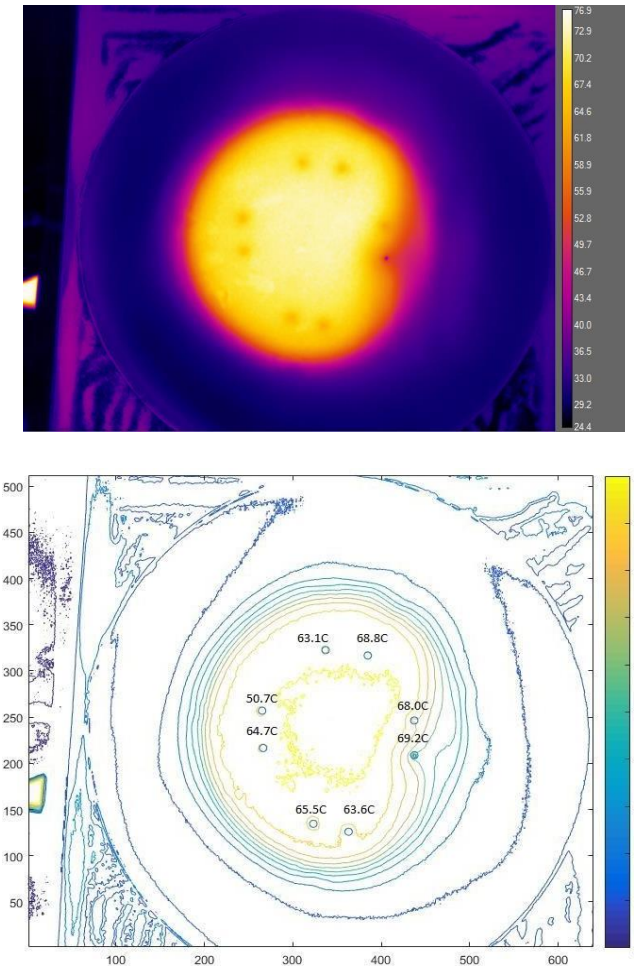

Figure -16

2-2-7) Using infrared bulb

To achieve a uniform temperature on the surface of the sand, an infrared bulb was utilized in the next step. It was hypothesized that due to the centralization of heater wires within the infrared bulb, this type of heater would produce a more uniform temperature. However, as shown in Fig17, the distribution of light and heating was not uniform when using infrared bulbs.

To address this issue and achieve a uniform temperature on the surface, a cylindrical shape made of aluminum foil was constructed and placed around the infrared bulb (Fig18). This device ensured that the infrared rays encountered the shiny surface of the aluminum multiple times before reaching the sand surface, causing them to reflect randomly. The random reflections resulted in a uniform distribution of infrared rays and heating. Consequently, a uniform heat flux was achieved, leading to a uniform temperature on the surface of the sand. After achieving a uniform heat flux, the use of the metal plate was no longer necessary. Therefore, it was removed from subsequent experiments to facilitate the easy evaporation of water vapor (in experiments involving wet sand) without altering its path. This is crucial for the numerical model, as the presence of the metal plate would change the vapor's trajectory, necessitating two-dimensional calculations for mass transfer.

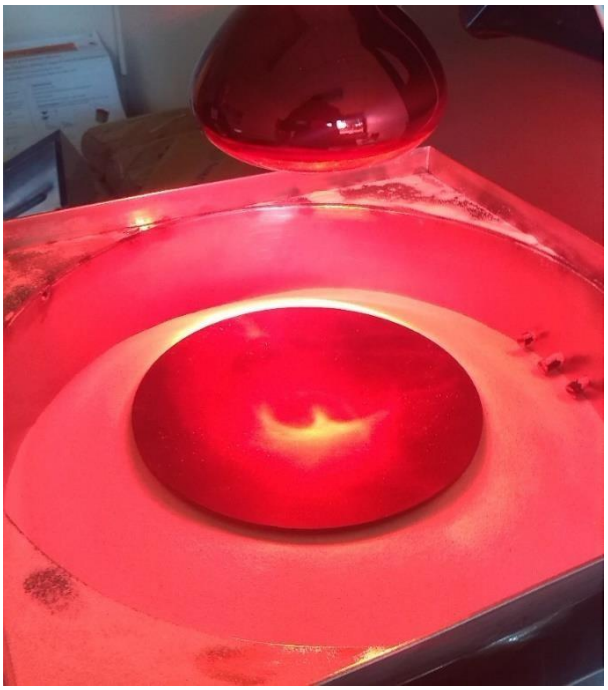

Figure -17

Figure -18

2-2-8) Dry & wet sand

The experimental part of the research was conducted in two parts:

In the first part, temperatures at different depths of dry sand were recorded. As explained in previous sections, achieving a uniform temperature on the surface was necessary to obtain useful data from the experiments. Subsequently, a series of experiments were conducted with dry sand.

The second part of the experiments involved measuring the temperature of wet sand at different depths and over time. The results in this part differed from those obtained with dry sand. The moisture inside the sand started to evaporate after reaching a specific temperature, and during this evaporation, the temperature of the sand increased very slowly. Contrary to expectations, the 100°C mark was not reached for the wet sand at different depths to become dry. The temperature of the wet sand approximately plateaued at around 60°C, and only after it had completely dried did the temperature begin to increase.

In the experiments with wet sand, 20 percent of the water needed to saturate the sand was always mixed. The volume of sand was calculated, and this volume was multiplied by the sand's porosity (0.4) to determine the volume of water required to saturate the sand. This amount was then multiplied by 0.2 to calculate the necessary volume of water for achieving the desired wet sand.

Mixing the required amount of water with dry sand is not an easy task, and to create a homogeneous wet sand mixture, the mixture must be thoroughly mixed for an extended period. Water tends to remain in certain areas between the sand grains, and redistributing it from wet areas to dry areas is challenging. It was discovered that using a device to spray water onto the dry parts of the sand instead of mixing water directly made it much easier to create a homogeneous wet sand mixture.

2-2-9) Testing the theoretical liquid fraction in wet sand

After mixing the appropriate amount of water with sand, an experiment was conducted to verify the accuracy of the predicted liquid fraction. It was suspected that some amount of water may have evaporated during the relatively long mixing process required to achieve a homogeneous wet sand mixture.

For this purpose, immediately after completing the mixing process, a sample of wet sand was taken. The sample was weighed and then placed in an oven to completely dry it. After drying, the dry sample was weighed again, and the difference between the two weights was calculated as the weight of water within the wet sand. The volume of water could be easily derived from this weight, and it was expected to be compared with the added water to the mixture to verify the accuracy of the assumed liquid fraction in the wet sand.

However, during this experiment, it was observed that the porosity of the wet sand always increased when attempting to take a sample. Consequently, due to the difference in porosity between the sample and the sand as a whole, even though the volume of water could be obtained, the correct liquid fraction of the wet sand after completing the mixing process could not be calculated. Therefore, it was not possible to test the accuracy of the theoretical liquid fraction in the wet sand.

2-2-10) Recording date

During the experiments, a data logger was occasionally used to record temperature instead of the LabView software. However, the recorded data curve was found to be discontinuous in the first probe, which was located on the surface and just below the black plate. This phenomenon was initially thought to be caused by the expansion of the metal and the friction between the probe and the metal, resulting in occasional disconnections between the probe and the plate. However, after testing various scenarios (such as increasing the thickness of the sand between the highest probe and the plate), it was determined that this issue was actually due to an internal problem with the data logger device. The expansion of the metal plate during heating could not cause such a phenomenon. As a result, for the remaining experiments, the LABVIEW software was used to record the data.

In the cylindrical box (2-2-2) shown in Figure 7, there are 10 probes inside the box. Two of these probes are located at the center of the box, while the others are positioned at the same radius from the center. This radius is smaller than the radius of the metal plate on the surface. The height of these probes was varied in different experiments. As expected based on the model shown in Figure 9, the temperature difference between the probes at the center and the other probes at the corners (with different heights) was much smaller than the temperature difference between the probes at the corners (with different heights). This indicates that the temperature at the center is higher than the temperature at the corners at the same level. The isothermal lines shown in Figure 9 have elliptical shapes.

3) Results

3-1) Dry Case

In the numerical model of this research, heat transfer for the dry case was modeled in two dimensions, considering the radius and depth, with the surface temperature as a constant boundary condition. Several experiments were conducted to achieve a uniform temperature on the surface. The method used to attain this condition is explained in section 2-2-7. The following section presents the experimental results (Figure 19) as well as the numerical results (Figure 20).

3-1-1) Experimental Result

For the most recent experimental result shown in Figure 19, a metal plate and cylindrical aluminum foil were utilized, and the temperature at different depths (z) and radii (r) was recorded over time.

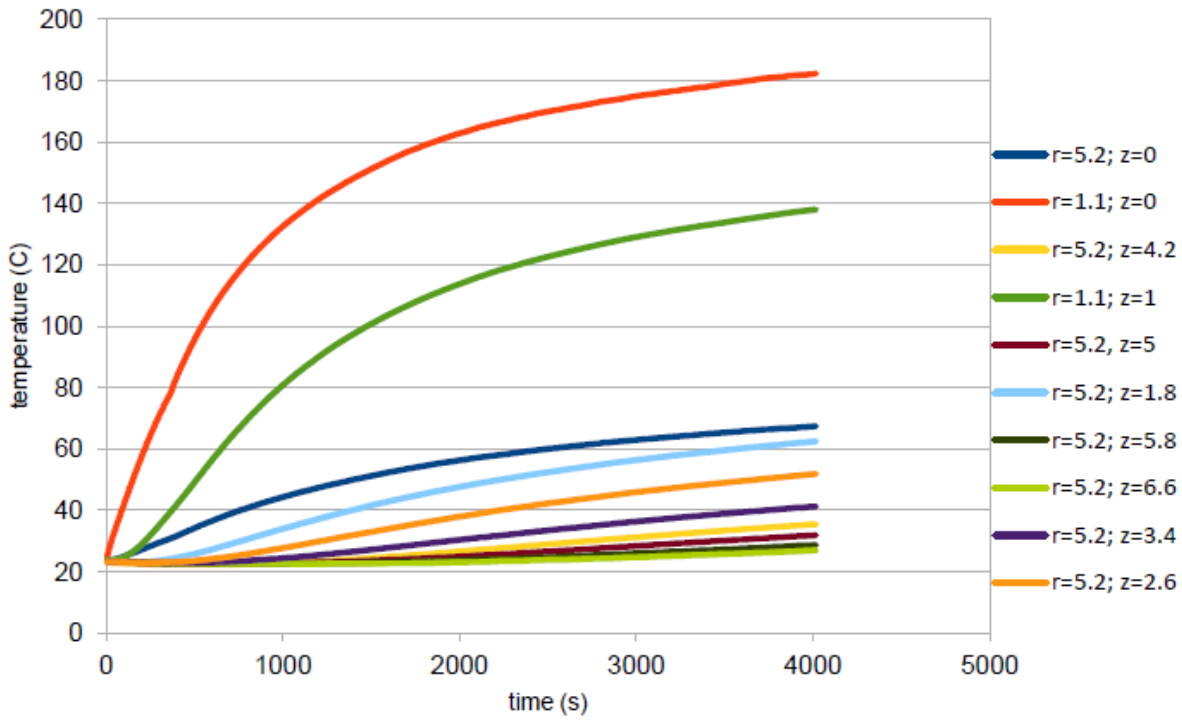

Figure -19

3-1-2) Slope of curves

In Figures 20 and 21, it is evident that the slope of the curves is initially high and decreases over time for all depths. The reason for this decrease can be understood by considering a thermocouple located just below the metal plate and in contact with the sand. At the beginning of the experiment, the temperature of this thermocouple is at its minimum. However, due to the high conductivity of the metal plate, as the temperature of the plate increases, the thermocouple temperature also increases at a similar rate, influenced by the infrared ray flux.

As time progresses, the rate of temperature increase in the metal plate decreases. Consequently, the rate of temperature increase in the first thermocouple also decreases. This results in a decrease in the slope of the first curve in Figure 19, as the slope is defined as the change in temperature (dT) over time (dt).

Regarding the second thermocouple, similar to the first one, its temperature is initially at its minimum. However, in this case, there is a layer of sand between the first and second thermocouples, which has lower conductivity compared to the metal plate. As a result, the temperatures in the first and second thermocouples do not increase at the same rate, and it takes some time for the heat to reach the second thermocouple from the first one.

Consequently, the curve of the second thermocouple (unlike the first one) reaches its maximum slope after a certain period of time. Beyond this point, the temperature difference between the first and second thermocouples decreases, and the rate of heat transfer between these two points also decreases.

$$\frac{q}{\Delta t} = \frac{\Delta T}{R.\Delta t}$$

We understand that the rate of heat transfer is directly related to the slope of the curve in Figure 19:

$$\frac{dq}{dt} = m.Cp\frac{dT}{dt} \;\&\; \frac{dT}{dt} = slope\ of\ curve$$

$\frac{dq}{dt}$ = the rate of heat transfer.
$m = mass.$
$Cp =$ Specific heat capacity.
T= temperature.
t=time

Therefore, the slope of the second curve in Figure 19 will decrease. This interpretation applies to the other probes at different depths as well. As the depth increases, the time required to reach the maximum slope in the respective curve will also increase, as can be observed in Figure 19.

If the experiment continues for a long period of time, the slope of the curves will approach zero, starting from the highest probe and gradually for the others.

3-1-3) numerical result

Regarding the numerical results, a two-dimensional model was used to calculate the temperature distribution in both the radial and depth directions. As mentioned in section 2-2-3, this was necessary because there are elliptical shapes for the isothermal lines within the sand, indicating that temperature changes with both radius and depth.

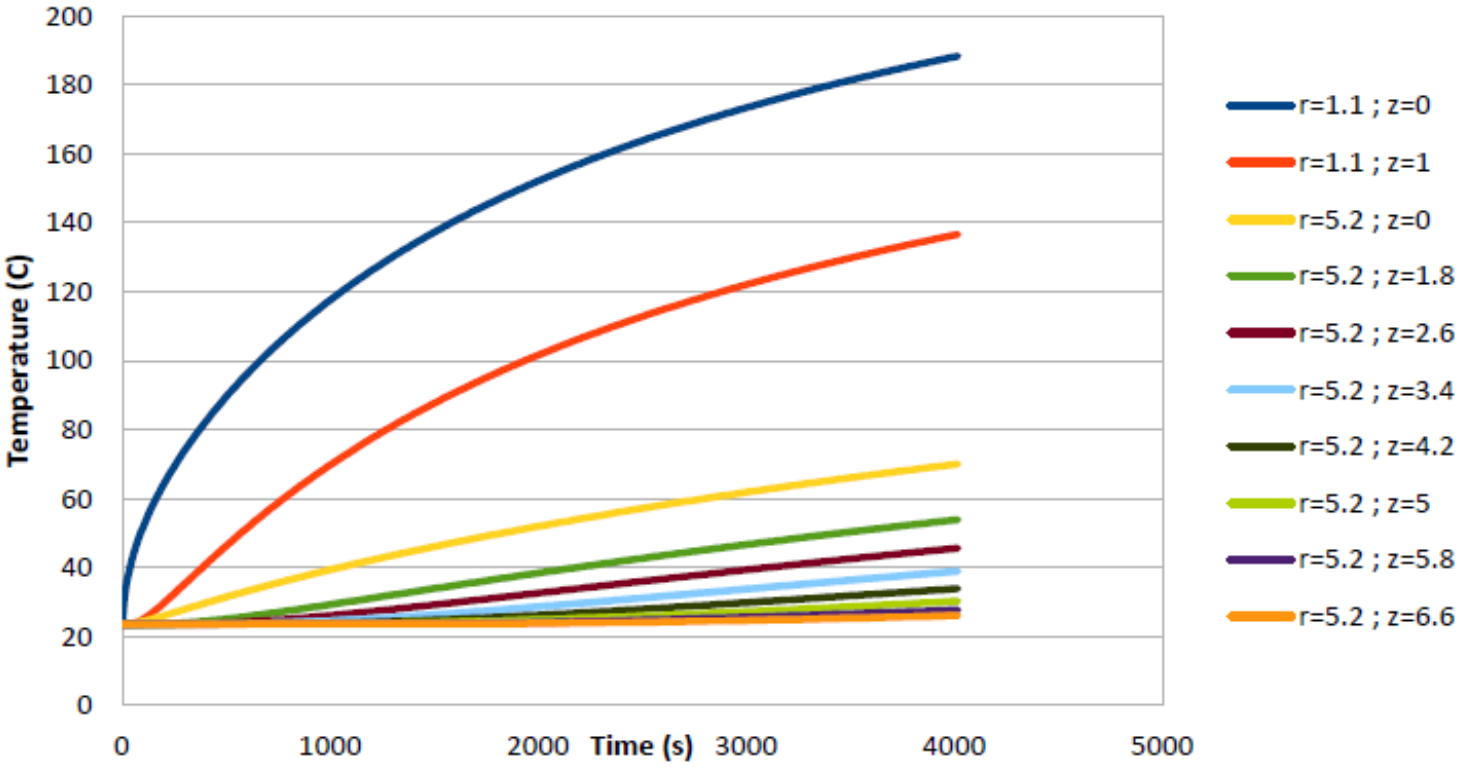
200
180
160
140
120
100
80
60
40
20
0
Temperature (C)
0
1000
2000
Time (s)
3000
4000
5000
r=1.1 ; z=0
r=1.1 ; z=1
r=5.2 ; z=0
r=5.2 ; z=1.8
r=5.2 ; z=2.6
r=5.2 ; z=3.4
r=5.2 ; z=4.2
r=5.2 ; z=5
r=5.2 ; z=5.8
r=5.2 ; z=6.6

Figure -20

3-1-4) ΔT between different thermocouples

Additionally, the temperature difference (ΔT) between different thermocouples remains constant when the heat transfer rate within the sand is relatively constant and the thermal conductivity of the porous media does not significantly change with depth and temperature. In such cases, the temperature difference will be the same for 1D heat transfer at different depths and distances.

$$q = \frac{\Delta T}{R}$$

$$R = \frac{L}{K.A}$$

$$q = \text{constant} \ \& \ R = \text{constant} \Rightarrow \Delta T = \text{constant}$$

The changes in temperature difference (ΔT) between different probes shown in Figures 19 and 20 are influenced by two main factors:

The heat transfer is not uniform in this scenario, as evident from the elliptical shape of the isothermal lines within the sand shown in Figure 9. Near the surface, the isothermal lines have an elliptical shape, while they become more similar to a hemisphere as you move further away from the surface. This variation in shape causes the temperature differences (ΔT) to change with depth.

The heat conductivity of the porous media (sand) increases with depth and temperature due to the expansion of air within the sand. To better understand the changes in heat conductivity in dry sand, conducting an experiment using one-dimensional heat transfer is suggested.

3-2) Humid case

The experiment was conducted using wet sand as described in section 2-2-8. One of the conditions in the humid case was to ensure that the vapor does not change its path within the sand. To achieve this, as mentioned in section 2-2-7, the metal plate was removed from the surface of the sand, and a cylindrical aluminum foil was used to generate a uniform heat flux (resulting in a uniform temperature).

3-2-1) Experimental results

There are considerations based on the arrangement of the probes. The radius of the cycle on which the probes are placed is not negligible compared to the radius of the heated part of the surface. Therefore, it can be concluded that a 2D heat transfer model is necessary for all these probes. However, for other probes located at the center of the box's cross-sectional area, it can be assumed that the heat transfer is one-dimensional. In this research, a 1D numerical model was used for the humid case, so to enable a comparison between the experimental and numerical results, the temperature readings from all probes far from the center in Figure 21 were excluded, and only the temperature data from two probes near the center were considered, as shown in Figure 22.

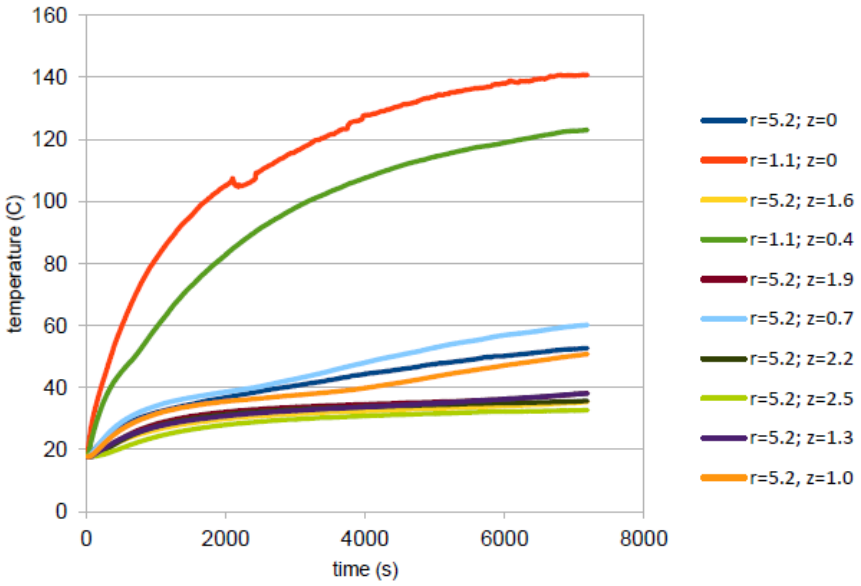

Figure -21

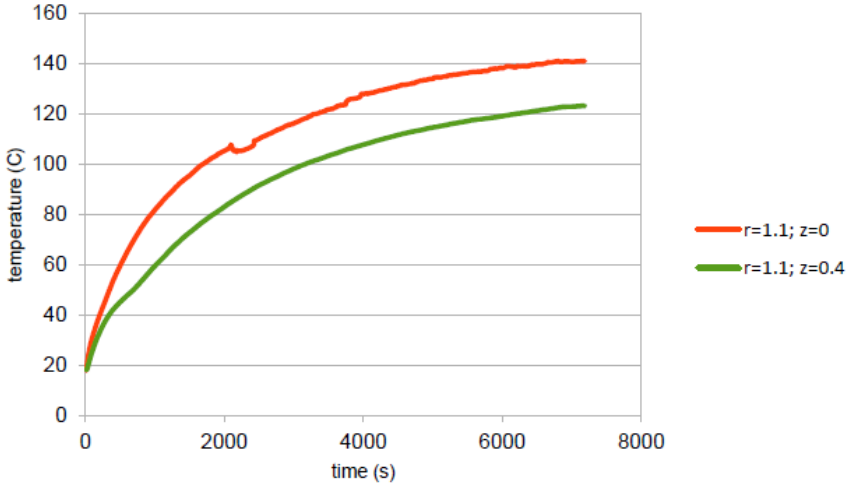

Figure -22

In Figure 21, the temperature difference between the probes represented by the red and green curves is significantly higher compared to the other probes. The red curve exhibits some irregular patterns that do not affect the lower curves. This irregularity is attributed to the use of a circular aluminum foil in the experiment, which was not in direct contact with the surface of the sand. This was done to prevent heat transfer from the aluminum to the sand. However, during the experiment, there was a short period of time when the hanging aluminum foil was moved due to blowing wind. It later returned to its original position. This immediate change in heat flux affected the temperature curve of the first probe (red curve) since its top was in direct contact with the surface of the sand. However, this event had a short duration and did not impact the lower layers of sand.

In the humid experiment, the distance between the depths of the probes was reduced in order to minimize the time required for the probes to reach a high temperature and for the sand to become completely dry. This is evident in Figure 21.

3-2-2) Regarding the presence of holes around the probes on the surface

it was observed after completing the humid experiments that some sand was removed in the surrounding areas of the probes. This phenomenon occurred multiple times during different experiments, as shown in Figures 23 and 24. Further research is needed to fully understand this phenomenon. However, it is evident that the vapor produced from the wet sand during heating traveled to the surface through these pathways. Additional experiments can determine if these pathways were created around the metal surface of all the probes, and if these pathways joined together as the length of each probe increased. Furthermore, it is essential to investigate why vapor is generated around the metal rods of the probes.

Figure -23

Figure -24

3-2-3) Numerical results

The results of the numerical model for the humid conditions, which were the same as the experiments described in section 3-2-1, are shown in Figure 25. In this figure, it can be observed that for each probe, there is an immediate increase in the slope of the curves after a certain time. This increase in slope occurs right after a section with the minimum slope.

The reason for this behavior can be explained by considering the process of evaporation in the wet sand. As time passes, the rate of evaporation in the wet sand starts to increase, leading to a gradual increase in temperature at a minimum rate, resulting in the minimum slope of the curves. The maximum rate of evaporation occurs when the sand reaches its maximum temperature (from the beginning of heating) and the maximum liquid fraction just before it becomes completely dry (as shown in section 1-3 and Figure 5). However, once the sand is completely dried, there is no more evaporation, causing the temperature to increase at a higher rate and the slope of the curves to increase immediately.

In Figure 25, it can be observed that the point at which the curve slope increases immediately is not the same for all the probes. This indicates that the sand at different depths will not dry at the same temperature. The reason for this variation is that, as mentioned in section 1-3 and Figure 5, the maximum liquid fraction just before the sand becomes completely dry increases for a specific period of time and then starts to decrease again.In our model, it takes a certain amount of time for the last probe to dry completely, and during this time, the maximum liquid fraction increases with depth. As a result, for the

probes at lower depths, there is a higher amount of maximum liquid fraction, which requires more time for all of this liquid fraction to evaporate. During this additional time, the temperature also reaches a higher value. Therefore, the point of immediate increase in slope will be at a higher temperature as we move towards the lower probes.

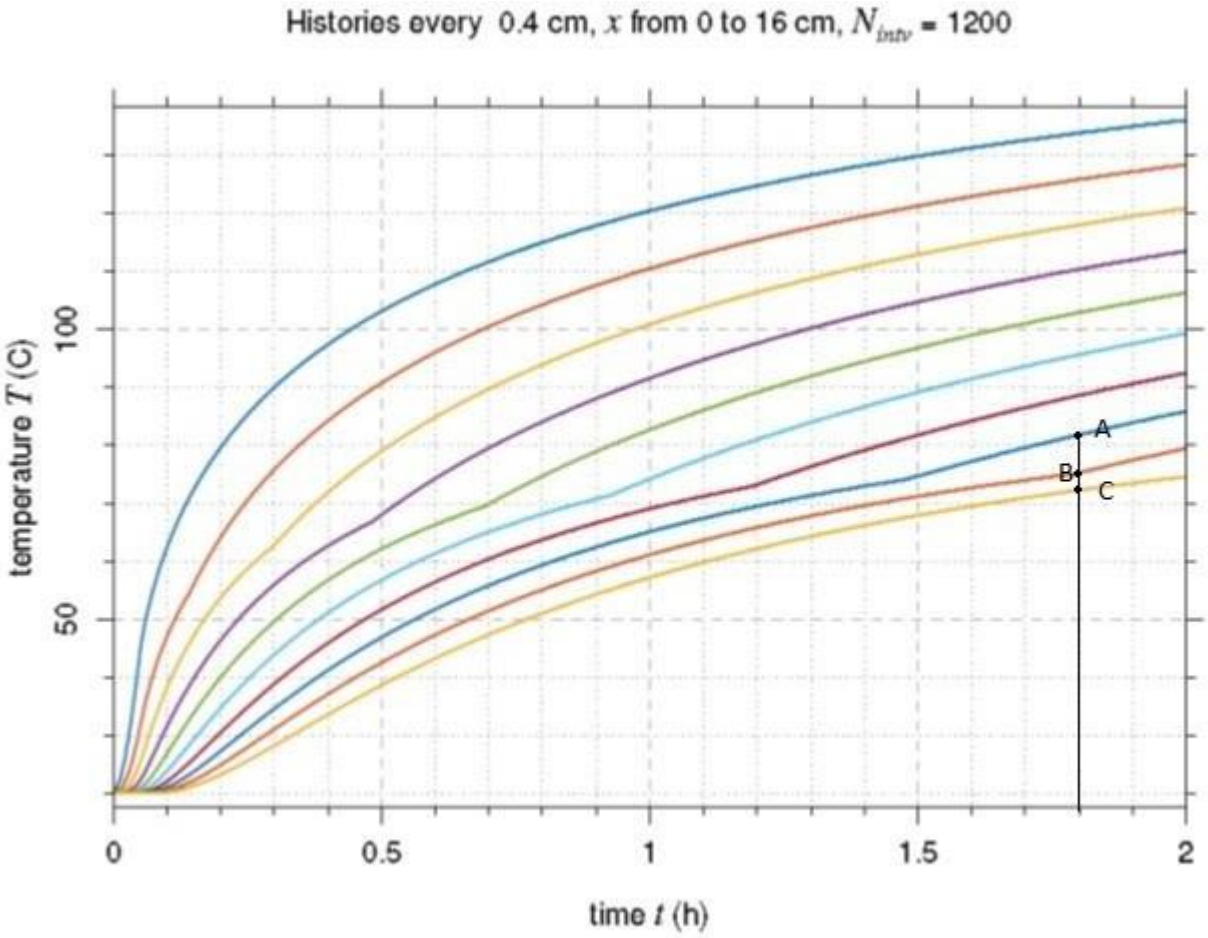

Figure -25

In Figure 25, after a sufficient amount of time has passed since the start of heating, when the slope of the curves is not very steep, a line was drawn at the point where the wet sand becomes completely dry (point "B"). This line represents a constant time. Since the liquid fraction at point "B" is at its maximum, the heat conductivity is also maximum. Therefore, point "B" on the upper curve is closest in distance to point "C" on the lower curve, which is within the wet part of the sand (resulting in the minimum temperature difference, denoted as ΔT, as explained in section 3-1-4). On the other hand, the distance (ΔT) between point "A" in the completely dry sand and point "B" reaches its maximum value because, at this time, all layers of sand between these points are dry and the thermal conductivity is minimum.

In terms of future work, the following perspectives are considered:

- The plan is to use a mixture of salt and sand to compare it with heating experiments conducted in the Atacama Desert in Chile, which has a soil that contains salt. This mixture can be either dry (composed of small grains) or humid (a combination of dry sand and brine).
- An experiment will be conducted to heat water-saturated sand or a two-layer porous medium consisting of a lower layer of water-saturated soil and an upper layer that is just wet.
- A two-dimensional code will be developed for heat transfer in humid porous media to compare with experimental results.
- Further investigation will be conducted to understand the reasons and conditions for the formation of a very thin layer of uniform temperature on the surface immediately after removing a non-homogeneous heat flux (as mentioned in section 2-2-6).
- The wet sand experiment will be conducted with a liquid fraction other than 20 percent saturation for a more comprehensive analysis.
- To better understand the changes in heat conductivity in dry sand, a one-dimensional heat transfer experiment is suggested (as described in section 3-1-4).
- Investigation will be carried out regarding the creation of holes on the surface of the sand during the humid experiments (section 3-2-2).

References

[1] E. Canot, R. Delannay, S. Mansour, EWGM: Evaporation in a Wet Granular Medium, presentation

[2] kurt Roth, soil physics, Lecture Notes, v2.2 (Autumn 2012)

[3] Salwa MANSOUR, Contribution to certain Physical and Numerical Aspects of the Study ofthe Heat Transfer in a Granular Medium, PhD thesis, UNIVERSITÉ DE RENNES 1, (2015)

[4] Mohamad Muhieddine, Edouard Canot, Ramiro March, Heat transfer modeling in saturatedporous media and identification of the thermophysical properties of the soil by inverse problem, Applied Numerical Mathematics 62 (2012) 1026–1040

[5] DIALLO Mamadou Saliou, Etude expérimentale du chauffage des sols humides, Master internship report, UNIVERSITÉ DE RENNES 1, (2016)

[6] Laura Pinzon Rincon, Imbibition et séchage d'un sol granulaire, Master internship report, UNIVERSITÉ DE RENNES 1, (2016)